CHAPTER 5

To investigate the effect of γ-Aminobutyric acid (GABA), Calorie Restriction (CR) and combination treatment on pancreatic β-cell proliferation in High-Fat Diet (HFD) + Streptozotocin (STZ) induced experimental mouse model.

To investigate the effect of γ-Aminobutyric acid (GABA), Calorie Restriction (CR) and combination treatment on pancreatic β-cell proliferation in High-Fat Diet (HFD) + Streptozotocin (STZ) induced experimental mouse model.

5.1 Introduction

Dysfunctional adipocytes and β-cells are involved in advancing obesity-induced T2D [Rathwa *et al.*, 2020]. Several aspects regulate the progression of T2D, such as excess calorie intake [Rathwa *et al.*, 2020; Pramanik *et al.*, 2018], genetic predisposition [Dwivedi *et al.*, 2011; Patel *et al.*, 2016; Palit *et al.*, 2020; Rathwa *et al.*, 2019] and sedentary lifestyle [Pramanik *et al.*, 2018], all of which contribute to persistent hyperglycemia and ultimately β-cell death. Even though there have been many recent management therapies for T2D, none can withstand the worsening condition of β-cell loss. Alternative remedies are proposed and tested that can replace β-cells from either stem cells or regenerate endogenous β-cells and sensitise insulin action in the peripheral tissues. CR, an effective dietary intervention for T2D, has been linked with longevity. CR reduces caloric intake, typically by 20-40% of ad libitum consumption, while preserving sufficient intake of protein and micronutrients to avoid malnutrition [López-Lluch *et al.*, 2016]. CR diminishes the degree of oxidative stress [Golbidi *et al.*, 2017; Picca *et al.*, 2015] and enhances the transcript levels of genes involved in mitochondrial function and biogenesis [Ben-Othman *et al.*, 2017]. It also improves insulin sensitivity, FBG and other cardiometabolic risk factors and reduces pro-inflammatory adipokines and total cholesterol [López-Lluch *et al.*, 2016; Golbidi *et al.*, 2017; Dogan *et al.*, 2017]. GABA has emerged as a new antidiabetic dietary supplement. It is a neurotransmitter secreted by the central nervous system (CNS) and pancreatic β-cells. It promotes protective and regenerative effects by reducing cell apoptosis and increasing β-cell replication rate [Wang *et al.*, 2019; Soltani *et al.*, 2011; Purwana *et al.*, 2014]. GABA exerts its action by two primary $GABA_A$ and $GABA_B$ receptors which regulate insulin and glucagon secretion in the pancreatic islets [Wang *et al.*, 2019]. GABA has shown its ameliorating effect by suppressing Treg cells in type 1 diabetes (T1D) [14]. Long-term therapy with GABA has demonstrated β-cell regeneration by proliferation or transdifferentiation [Ben-Othman *et al.*, 2017].

This study investigates the combinatorial effect of CR and GABA in the T2D mouse model induced by a high-fat diet (HFD) + streptozotocin (HFD+STZ). To evaluate the effect of CR and GABA on multiple targets and regulatory pathways, we assessed i) insulin sensitivity, glucose tolerance and metabolic profile, ii) transcript levels of key genes

involved in hepatic glucoregulation, lipid metabolism in adipose tissue (AT) and mitochondrial biogenesis in skeletal muscle (SK), iii) ETC complex I, II and III activities in SK, and iv) regenerative markers in β-cells.

5.2 Animals and experimental strategy

5.2.1 Animals

The experimental procedures were approved by the Institutional Ethical Committee for Animal Research (IECHR), Faculty of Science, The Maharaja Sayajirao University of Baroda, Vadodara, Gujarat, India (FS/IECHR/2016-9). Male C57BL/6 mice (~8-10 weeks old, approximately 20-22 grams) were procured from ACTREC, Mumbai. They were housed in our animal house at 23.0±1°C with a 12-hrs light/dark cycle and acclimatised for one week. These animals had free access to standard chow/HFD/CR diet (Keval Sales Corporation, Vadodara, India) and water.

5.2.2 Development of T2D mouse model

The mice were divided into two groups. The control group (n=6) was fed with a normal chow diet (NCD). Obesity can induce multiple damaging effects on peripheral tissues. Working on similar lines, mice (n=25) were fed with HFD for 20 weeks to induce obesity and insulin resistance. After 20 weeks, these mice received three consecutive doses of 40 mg/kg BW STZ i.p. (MP Biomedicals, India) to induce β-cell loss. The HFD+STZ model is characterised by a significant increase in body weight (≥30 grams), hyperglycemia (FBG ≥300 mg/dL), hyperlipidemia, insulin resistance and β-cell loss [Bansal *et al.*, 2012].

5.2.3 Treatment

The HFD+STZ treated animals were divided randomly into four groups (4-5 mice/group): 1) Diabetic control (HFD+STZ) 2) CR diet-fed (30% reduction of HFD) [Huang *et al.*, 2010; Fontana *et al.*, 2015] 3) GABA treated (2.5 mg/kg bw i.p.) (Sigma–Aldrich, United States) [Ben-Othman *et al.*, 2017] and 4) CR+GABA treated. Treatment was given daily for five weeks along with 100 mg/kg bw i.p. BrdU (MP Biomedicals, India) on alternate days. CR diet comprised of 39% casein, 21% lard, 19 % sucrose, 16% vitamin-mineral premix, and 5% cellulose. The timeline is shown in figure 5.1.

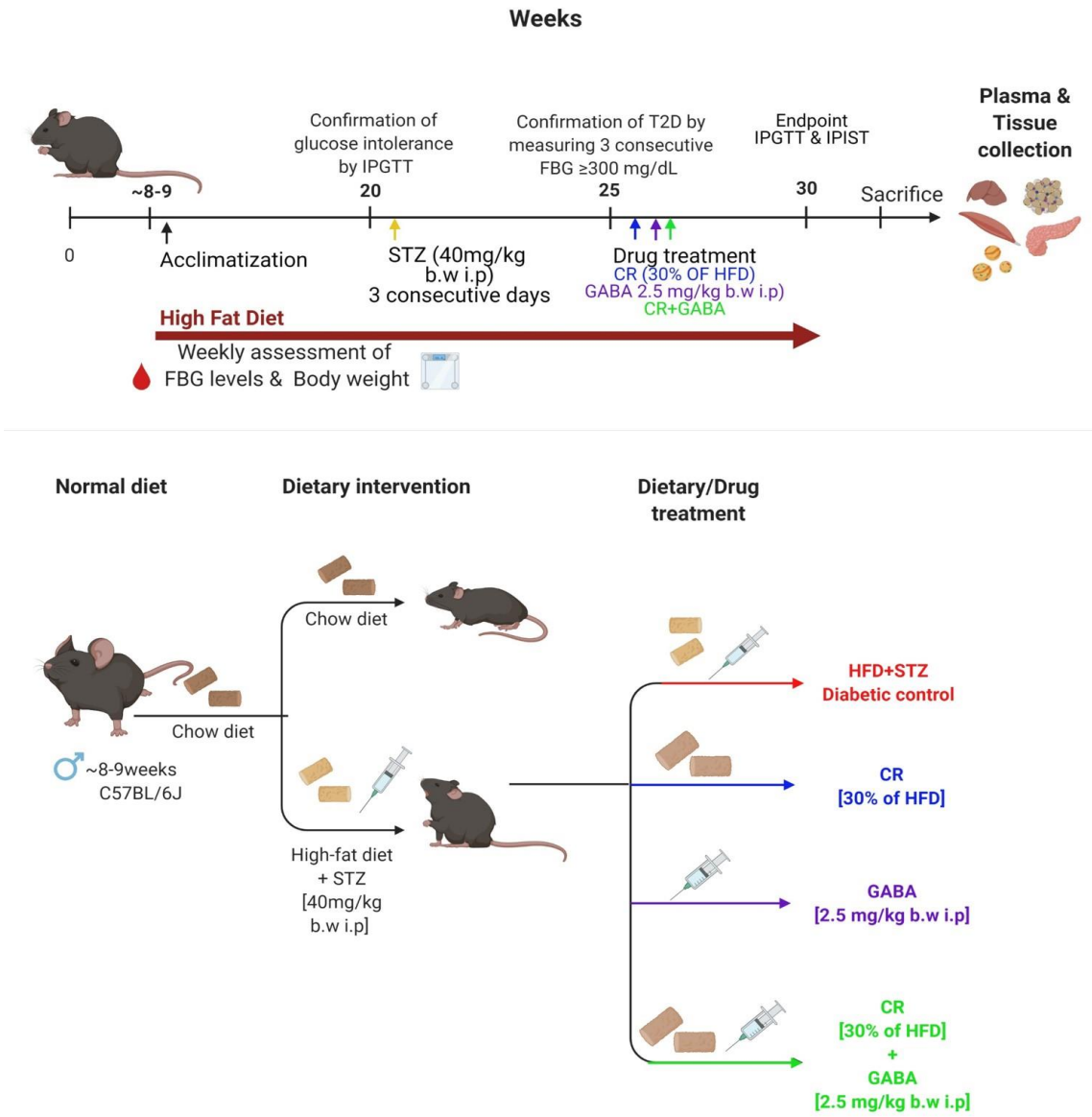

Figure 5.1. The experimental timeline: ~8-9 weeks old male C57BL/6 mice were procured and subjected to 1 week acclimatization. 25 of them were fed with HFD for 20 weeks to induce obesity and insulin resistance while 6 were fed with chow diet. Food intake, water consumption, BW and FBG levels were monitored weekly. After 20 weeks, the HFD fed mice received three consecutive doses of STZ (40 mg/kg i.p.) to induce β-cell loss. Once obesity induced T2D was confirmed, these animals were divided randomly into four groups, for 6 weeks drug treatment. Post treatment, IPGTT and IPIST were carried out, the animals were sacrificed, and tissues were harvested for further analysis.

5.2.4 Metabolic and Biochemical Parameters

5.2.4.1 Metabolic profiling

FBG was measured weekly using glucometer by tail snipping (TRUEresult, Nipro, India) along with monitoring BW as well as food and water intake. At the end of the experiment, 1 ml of blood was collected from the orbital sinus for the biochemical assays after 5 hrs of

fasting. Plasma was separated and used for assessing lipid profile [total cholesterol (TC), triglycerides (TG) and high-density lipoprotein (HDL)] by using commercial kits (Reckon Diagnostics P. Ltd, India). Friedewald's (1972) formula was used for calculating low-density lipoprotein (LDL).

5.2.4.2 Intraperitoneal Glucose Tolerance Test (IPGTT) and Intraperitoneal Insulin Sensitivity Test (IPIST)

We have evaluated glucose tolerance and insulin sensitivity by IPGTT and IPIST at the end of 6 weeks of drug treatment. Mice were fasted for 6 hrs and injected with glucose (2g/kg BW i.p.) or insulin (0.5U/kg BW i.p.) for IPGTT and IPIST [6], respectively. Blood glucose levels were measured by glucometer at the specified time points 0, 30, 60, 90, and 120 mins after glucose or insulin injections.

5.2.4.3 Assessment of Insulin and C-peptide levels

The plasma levels of insulin and C-peptide in the experimental animals were measured using commercial ELISA kits (RayBio, USA).

5.2.5 Gene expression profiling

After sacrificing the mice, peripheral tissues liver, AT and SK were dissected and stored in RNAlater™ Stabilization Solution (Thermo Fisher Scientific, USA). Total RNA was extracted by the Trizol method as described previously [7]. The mRNA expression of targeted genes and *GAPDH* were monitored by LightCycler®480 Real-time PCR (Roche Diagnostics GmbH, Germany) using gene-specific primers (Eurofins, India) [Table 5.1]. Expression of *GAPDH* gene was used as a reference. Real-time PCR was performed as described previously [8].

Table 5.1 Primers used for the transcript analysis.

Gene Primer	**Sequence (5'to 3')**	**Annealing Temperature**	**Amplicon Size (bp)**	**Tissue**
Glucokinase	**FP:** AGGAGGCCAG TGTAAAGATGT **RP:** TCCCAGGTCT AAGGAGAGAAA	56°C	90bp	Liver
PEPCK	**FP:** CTGCATAAC GGTCTGGACTTC **RP:** CAGCAAC TGCCCGTACTCC	65°C	151bp	
G6Pase	**FP:**CTGTTTGGACAAC GCCCGTAT **RP:**AGGTGACAGG	56°C	91bp	

	GAACTGCTTTA			
Glut2	**FP:**CTTGGAAGGATC AAAGCAATG **RP:**CAGTCCTGAA ATTAGCCCAC	60°C	150bp	
Glycogen Synthase	**FP:**ACCAAGGCCA AAACGACAG **RP:**GGGCTCACAT TGTTCTACTTG	61°C	102bp	
Glycogen Phosphorylase	**FP:** GAGAAGCGAC GGCAGATCA **RP:** CTTGACCAGA GTGAAGTGCA	65°C	102bp	
SIRT-1	**FP:** GATGAAGTTG ACCTCCTCA **RP:**GGGTATAGAAC TTGGAATTAG	64°C	86bp	Liver, SK
PGC-1α	**FP:** AGCCGTGACCA CTGACAACGA **RP:** GTAGCTGAGCT GAGTGTTGGC	69°C	129bp	
TFAM	**FP:**CTGAGGAAAAGC AGGCATA **RP:**ATGTCTCCGGAT CGTTTCAC	69°C	142bp	
ATGL	**FP:**TGTGGCCTCAT TCCTCCTAC **RP:**TCGTGGATGTTG GTGGAGCT	61.8°C	158bp	AT
ACC-1	**FP:** ACGCTCAGGTC ACCAAAAAGAAT **RP:** GTAGGGTCCCG GCCACAT	57°C	70bp	
GAPDH	**FP:** AGGTCGGTGTG AACGGATTTG **RP:**TGTAGACCAT GTAGTTGAGGT	56°C	123bp	Liver, SK, AT

FP: Forward Primer; RP: Reverse Primer; bp: base pair; SK: Skeletal Muscle; AT: Adipose Tissue

5.2.6 Estimation of Oxygen Consumption Rate (OCR)

Skeletal muscle was isolated from left thigh of the mouse and mitochondria were isolated by mitochondria isolation kit (Thermo Scientific TM, Catalog no. 89801). The isolated mitochondria were resuspended in mitochondria respiration buffer (80 mM KCl, 0.1% BSA, 50 mM HEPES, 2 mM $MgCl_2$, and 2.5 mM KH_2PO_4; pH 7.2). Outer membrane integrity of the isolated mitochondria was evaluated by impermeability to exogenous cytochrome c which

was constantly >95%. The activities of respiratory chain complexes I-III were recorded using 100 mM Pyruvate & 800 mM Malate (complex I), 1M Succinate (complex II) and 10 mM α-glycerophosphate (complex III), and the protein concentration was estimated by the Bradford method (Stoscheck *et al*., 1990). OCR was determined by measuring the amount of oxygen (nmol) consumed, divided by the time elapsed (min) and the amount of protein present in the assay (Li and Graham, 2012).

5.2.7 Pancreatic tissue preparation, Immunohistochemistry (IHC), Assessment of β-cell regeneration and apoptosis

At the end of experiment, animals were sacrificed, and pancreatic tissues were fixed in 10% formalin and were processed for paraffin embedding. 5µm sections were cut from the paraffin-embedded blocks. To perform IHC, these sections were deparaffinised in100% xylene and washed serially in ethanol grades (100%, 95%, 80% and 70%) and proceeded with an antigen retrieval step (1N HCl at 37°C for 45 min). Subsequently, these sections were blocked with 5% donkey serum made in phosphate buffer saline (PBS) [Jackson ImmunoResearch Laboratories, Inc. USA], and antibodies were diluted in the blocking reagent. The details of the antibodies are as indicated in Table 5.2. The sections were incubated with primary antibody for one hour at 37°C, washed with PBS, and incubated with secondary antibody for 45 min at 37°C. These sections were stained with anti-fade DAPI (Thermo Fisher Scientific, USA). The sections were covered with a coverslip. The sections were visualised under a confocal microscope (ZEISS LSM, Oberkochen, Germany) at 60X, and the images were processed by Image J (NIH, USA). Immunofluorescence staining (IFS) with anti-insulin and anti-BrdU was used to monitor β-cell proliferation. IFS with anti-insulin, anti-PAX-4 (paired box gene 4), and anti-ARX (Aristaless Related Homeobox) was carried out for α-cell to β-cell transdifferentiation while anti-insulin, anti-NGN-3 (Neurogenin 3) and anti-PDX-1 (pancreas/duodenum homeobox protein 1) were considered for β-cell neogenesis. IFS anti-insulin and TUNEL/anti-AIF (Apoptosis Inducing Factor) monitored β-cell death. Results obtained were expressed as the percentage of specified markers for regeneration and death.

Table 5.2 Antibodies used for the IHC studies.

Primary Antibody	Secondary Antibody	Excitation (nm)	Emission (nm)
Anti-Insulin (1:100, Guinea Pig) [DAKO Agilent, USA]	Alexa 488 (1:500, Donkey) [Jackson ImmunoResearch Laboratories, Inc. USA]	493	519

NGN3 (1:50, rabbit) [Thermo Fisher Scientific, USA]	Alexa 647 (1:500, Donkey) [Jackson ImmunoResearch Laboratories, Inc. USA]	651	667
ARX (1:500, Rabbit) [Sigma-Aldrich, Germany]			
Anti-Glucagon (1:200, rabbit) [Cell Signaling Technology, USA]			
Anti-AIF (1:400, rabbit) [Thermo Fisher Scientific, USA]			
PDX-1 (1:1000, Goat) [Abcam, USA]	Rhodamine Red (1:200, Donkey) [Jackson ImmunoResearch Laboratories, Inc. USA]	570	590
PAX-4 (1:500, Goat) [Sigma-Aldrich, Germany]			
BrdU (1:100, Goat) [Abcam, USA]	Rhodamine Red (1:200, Rat) [Jackson ImmunoResearch Laboratories, Inc. USA]	570	590

5.2.8 Statistical analyses

The data was analysed and expressed as the mean ± SEM, and $p<0.05$ was considered statistically significant. The inter-group analysis was carried out by one-way ANOVA, followed by Tukey's test for multiple group analysis. All the estimations from plasma were carried out in duplicate to ensure the coefficient of variation (CV) is below 10%. All the analyses were carried out using the Prism software 6 (GraphPad Prism, San Diego, CA, USA).

5.3 Results: HFD+STZ induced T2D mouse model establishment.

After 20 weeks of HFD treatment, animals became obese and insulin resistant. There was significant increase in BW (Figure 5.2 A-B). After two weeks of STZ administration followed by HFD treatment, mice became hyperglycemic as indicated by FBG levels ≥300 mg/dL (Figure 5.2 C-D).

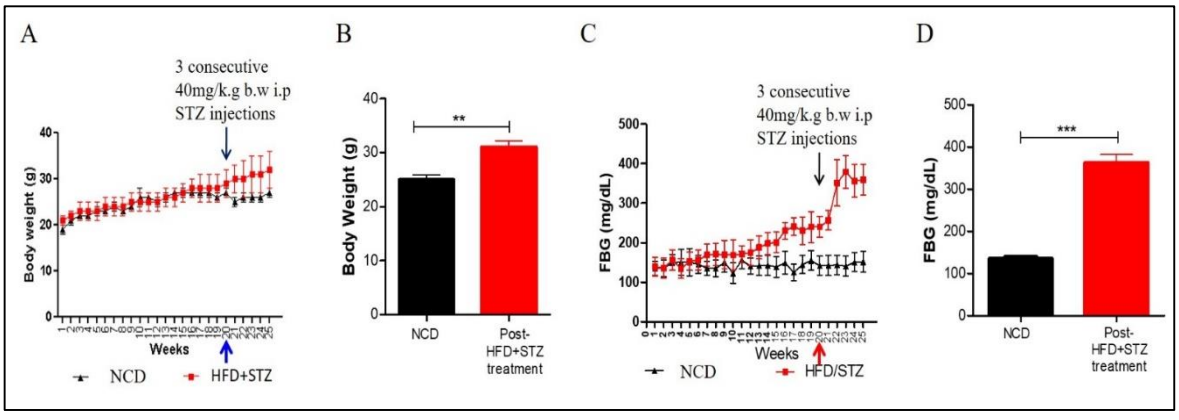

Figure 5.2 (A-D) Body weight and fasting blood glucose levels in experimental diabetic mice (Control and post- HFD+STZ treatment). A significant difference in BW and FBG was observed in the animals before and after HFD+STZ treatment. (**p<0.01, ***p<0.001 respectively) (Control, n=5 and post HFD+STZ, n=25).

5.3.1 Metabolic and Biochemical Assessment

5.3.1.1 Metabolic profiling

GABA treated group showed significant reduction in FBG levels (p<0.01), but no change was observed in BW, while CR monotherapy showed improvement in BW (p<0.05) but not in FBG levels. The BW (p<0.05) and FBG (p<0.01) levels of the CR+GABA treated group were significantly reduced at the end of 5 weeks of treatment compared to the HFD+STZ group as shown in Figure 5.3.

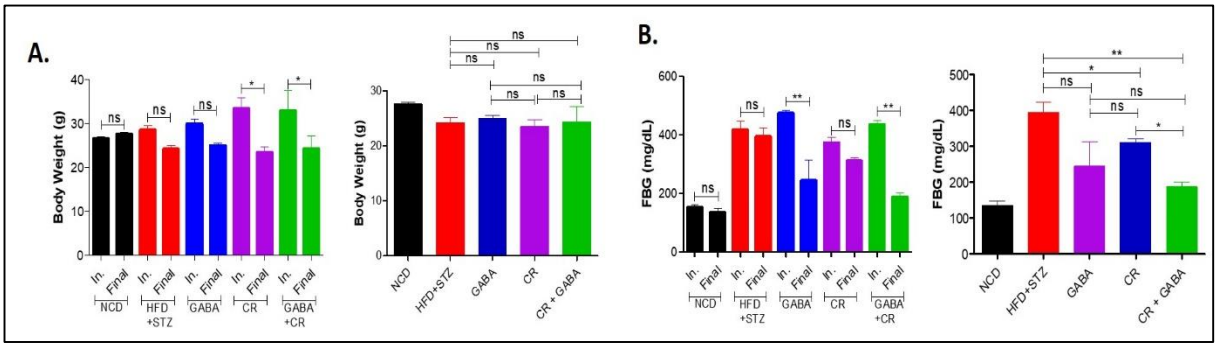

Figure 5.3 Body weight and fasting blood glucose levels. A) A significant decrease in BW was observed in the CR and CR+GABA treated groups compared to HFD+STZ. B) FBG levels in GABA and CR+GABA treated groups showed significant reduction compared to HFD+STZ (ns=non-significant, *p=0.05; **p<0.01, n=4-5/group).

5.3.1.2 Lipid profiling

The GABA treated group showed no significant difference in lipid profile (p>0.05), while CR fed mice (p<0.05) showed reduced TG levels as compared to the HFD+STZ group. TC, TG and LDL levels were significantly reduced in the CR+GABA treated group (p<0.05) as compared to the HFD+STZ group (Figure 5.4).

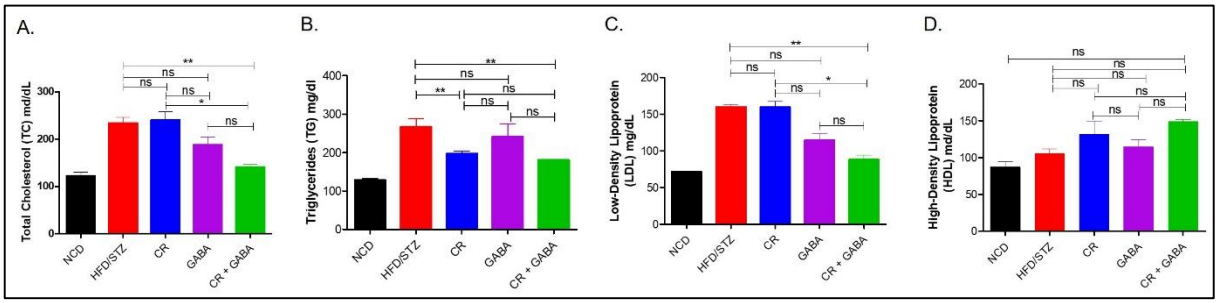

Figure 5.4 Plasma lipid levels. A-D) TC, TG, & LDL levels were reduced in CR+GABA group as compared to HFD+STZ group while no difference was observed in the rest of the

treated groups (ns=non-significant, *p<0.05, **p<0.01, vs HFD+STZ; $^{@}p$<0.05, $^{@@}p$ <0.01 vs NCD; $^{\#}p$<0.05, vs CR n=4-5/ group).

5.3.1.3 Glucose Tolerance and Insulin Sensitivity

To further test our hypothesis, we performed IPGTT and IPIST post-treatment. CR monotherapy did not show improvement in glucose tolerance and insulin sensitivity. GABA (p<0.05) and CR+GABA (p<0.01) treated groups showed a significant decrease in blood glucose levels by 120 mins as compared to HFD+STZ group (Figure 5.5A). The AUC plot showed significant increase in glucose tolerance in GABA and CR+GABA treated groups (p<0.05) (Figure 5.5B). CR+GABA (p<0.01) treated group showed improved insulin sensitivity as blood glucose levels were reduced to normoglycemia by 120 mins as compared to HFD+STZ group (Figure 5.5C & D).

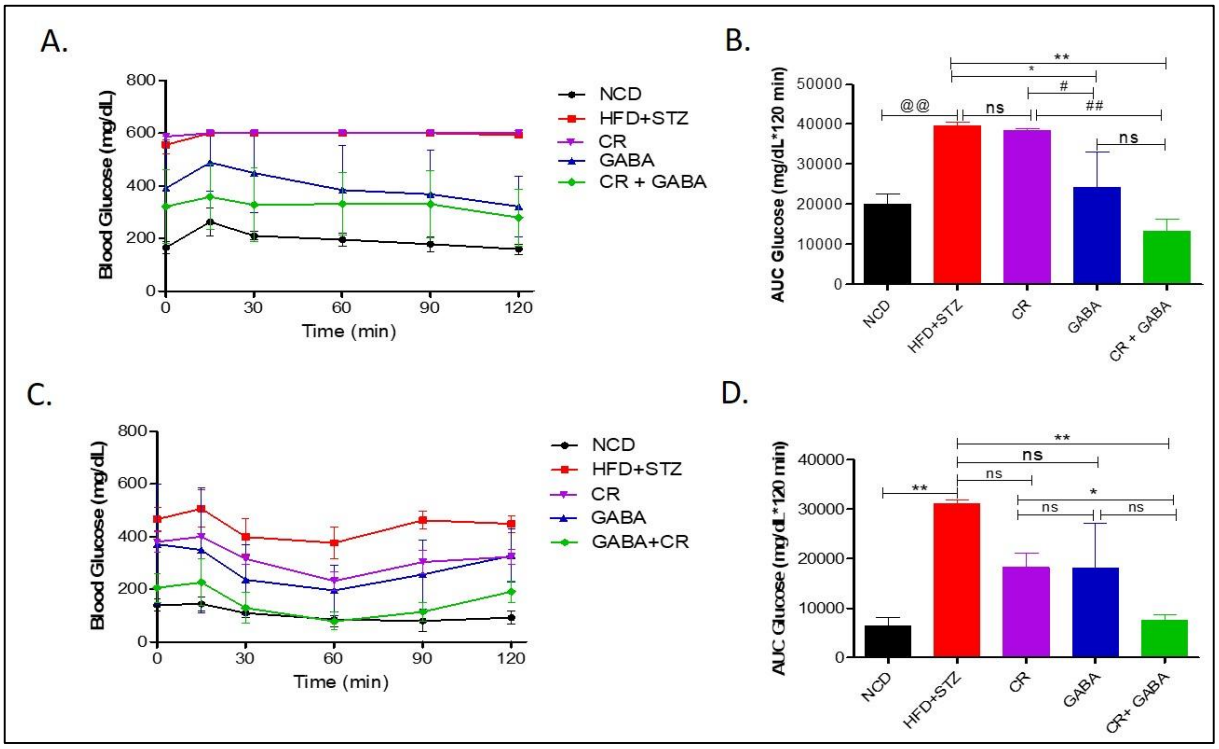

Figure 5.5 IGTT and IPIST. A) Blood glucose levels in the GABA and CR+GABA groups were significantly lower than CR and HFD+STZ mice at 60, 90 and 120 mins of glucose administration. B) AUC 0–120 curve indicated improved glucose tolerance in the GABA and CR+GABA treated groups compared to the HFD+STZ group. C) Blood glucose levels in CR+GABA were significantly lower than in CR, GABA and HFD+STZ mice at 60, 90 and 120 mins of insulin administration. D) AUC 0–120 curve in mice treated with CR+GABA was significantly lower than in HFD+STZ group. (ns=non-significant, *p<0.05, **p<0.01, ***p<0.001 vs HFD+STZ; $^{@}p$<0.05, $^{@@}p$ <0.01 vs NCD; $^{\#}p$<0.05, $^{\#\#}p$ <0.01 vs CR n=4-5/ group).

5.3.1.4 Insulin and C-peptide levels

Significant increase in insulin and c-peptide levels along with improved insulin/c-peptide ratio was observed in GABA & CR+GABA (p<0.05) treated groups as compared to HFD+STZ group (Figure 5.6 A-C). No significant difference was observed in CR group.

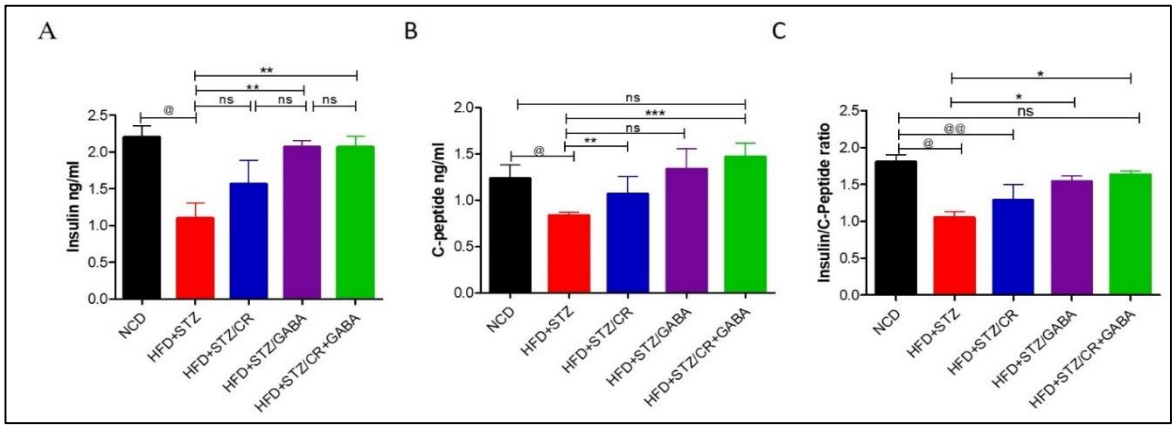

Figure 5.6 Plasma insulin, c-peptide levels and insulin/c-peptide ratio. (A & B) Increased insulin and c-peptide levels were observed in GABA & CR+GABA treated groups as compared to HFD+STZ. C) Significant increase in insulin/c-peptide ratio was observed in GABA & CR+GABA treated groups as compared to HFD+STZ group (ns=non-significant, *p<0.05, **p<0.01, ***p<0.001 vs HFD+STZ; $^{@}p$<0.05, $^{@@}p$ <0.01 vs NCD; n=4-5/ group).

5.3.2 Gene expression profiles

GABA treated group showed significant decrease (p<0.05) in the expression of *phosphoenolpyruvate carboxykinase* (*PEPCK*-gluconeogenesis), glucose-6 phosphatase (*G6Pase*), and *glycogen phosphorylase* (*GP*-glycogenolysis) in liver (Figure 5.7). However, there was no significant difference in the expression of *adipose triglyceride lipase* (*ATGL*-lipolysis) and *acetyl-CoA carboxylase-1* (*ACC-1*-lipogenesis) in adipose tissue (p>0.05) (Figure 5.8). Also, there was no significant difference observed in *sirtuin-1* (*SIRT-1*), *PPARG coactivator 1-α* (*PGC-1α*), and *transcription factor A mitochondrial* (*TFAM*-mitochondrial biogenesis) transcript levels in skeletal muscle (p>0.05) (Figure 5.9). CR fed mice showed significant decrease (p<0.05) in the expression of *G6Pase*, *PEPCK* (gluconeogenesis), *GLUT2* and *GP* (glycogenolysis) in liver (Figure 5.7). However, there was no significant difference observed in the expression of *ATGL* and *ACC-1* in adipose tissue of CR fed mice (p>0.05) (Figure 5.8). Further, CR fed mice showed significant increase (p<0.05) in *PGC-1α* transcript levels in skeletal muscle (Figure 5.9). CR+GABA treated group showed significant decrease (p<0.05) in the expression of *G6Pase*, *PEPCK* (gluconeogenesis), *GLUT2* and *GP* (glycogenolysis) genes, and significant increase (p<0.05) in *glucokinase* (glycolysis) expression (Figure 5.7). Interestingly, lipogenesis got

up-regulated as marked by the increased *ACC-1* expression. Consequently, as a compensatory mechanism, lipolysis was also up-regulated, as observed by the increased *ATGL* expression (p<0.05) (Figure 5.8). CR+GABA treated group also showed significant increase (p<0.05) in *SIRT-1*, *PGC-1α* and *TFAM* transcript levels in skeletal muscle (Figure 5.9).

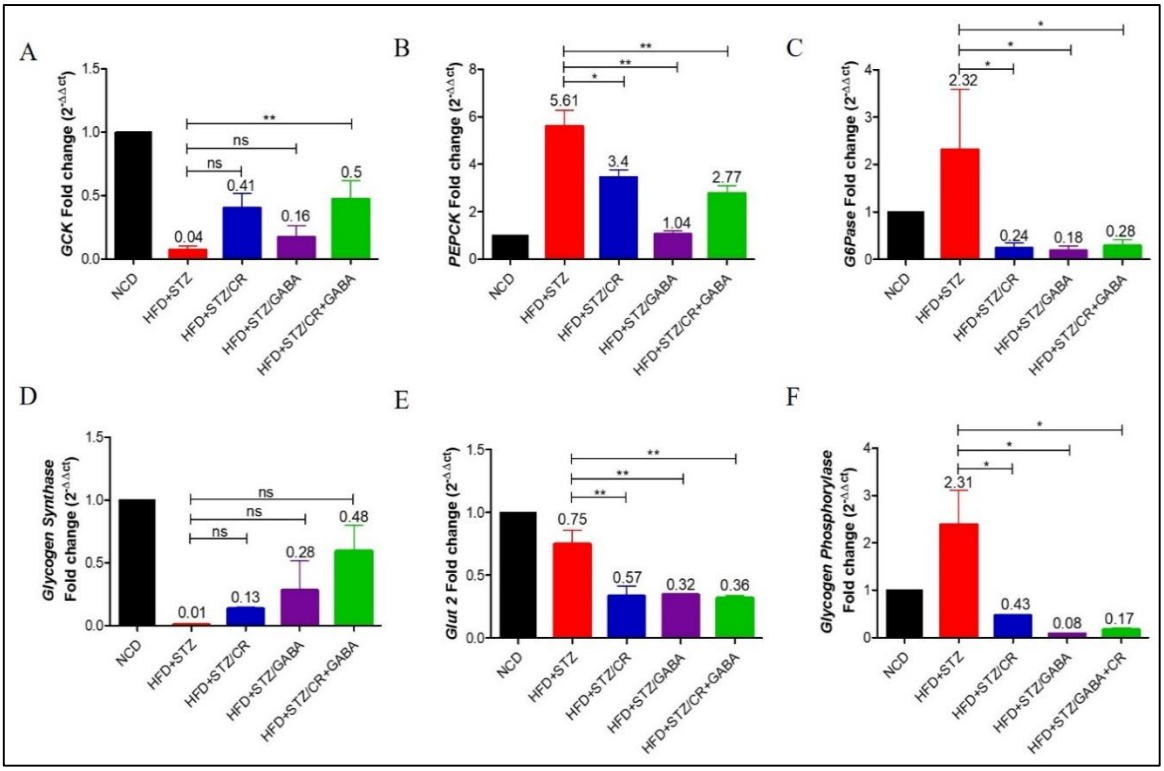

Figure 5.7 Transcript levels of glucoregulatory enzymes in liver: A. *GCK* fold change. After normalisation with GAPDH expression, a 0.5-fold increase in *GCK* transcript levels was observed in CR+GABA group as compared to HFD+STZ group. **B & C. Fold change in *PEPCK* & *G6Pase***. GABA, CR and CR+GABA showed a significant 1-fold, 3-fold and 2.7 fold decrease in *PEPCK*. GABA, CR and CR+GABA showed a significant 0.18-fold, 0.24-fold and 0.28-fold decrease in G6Pase expression compared to the HFD+STZ group. **D-E.*Glycogen synthase, GLUT2* fold change**. No significant change was observed in *glycogen synthase*, whereas *GLUT2* expression was significantly decreased in all the treated groups compared to HFD+STZ group. **F. Fold change in *Glycogen phosphorylase***. A significant 0.08-fold, 0.43-fold and 0.17-fold reduction in *glycogen phosphorylase* expression was observed in the monotherapies and combination groups compared to HFD+STZ group. (ns=non-significant, *p<0.05, **p<0.01; ***p<0.001, n=4-5/group).

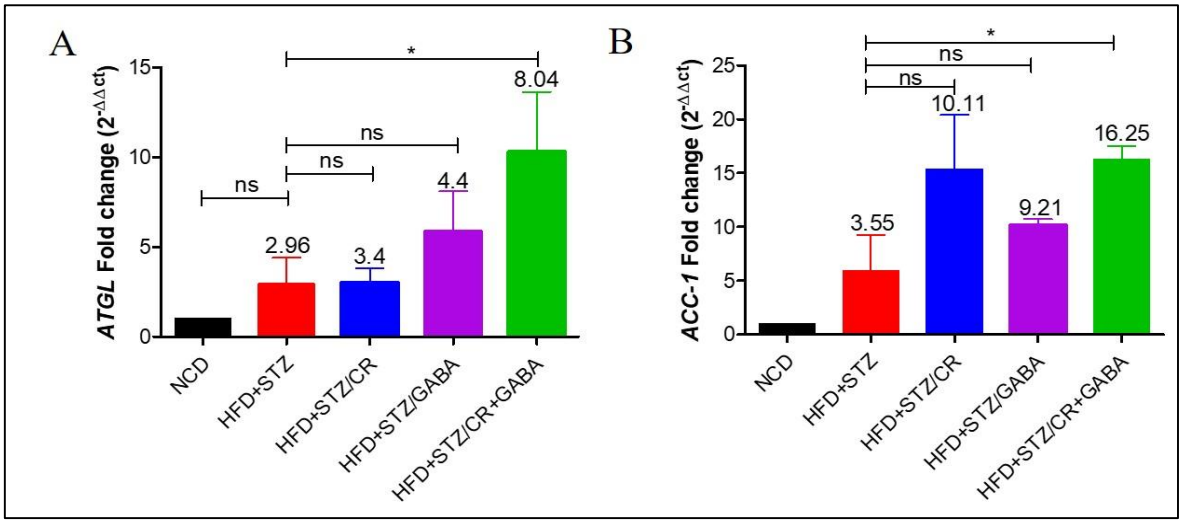

Figure 5.8 Transcript levels of lipid metabolism markers in the adipose tissue. A) Fold change in ***ATGL* mRNA**. A significant 8-fold increase in *ATGL* expression was seen in the CR+GABA group as compared to HFD+STZ group. B) Fold change in ***ACC-1* mRNA**. A significant 16-fold increase in *ACC-1* expression was seen in CR+GABA group compared to HFD+STZ group. (**p*<0.05, ns=non-significant; *p*>0.05) (n=4-5/group).

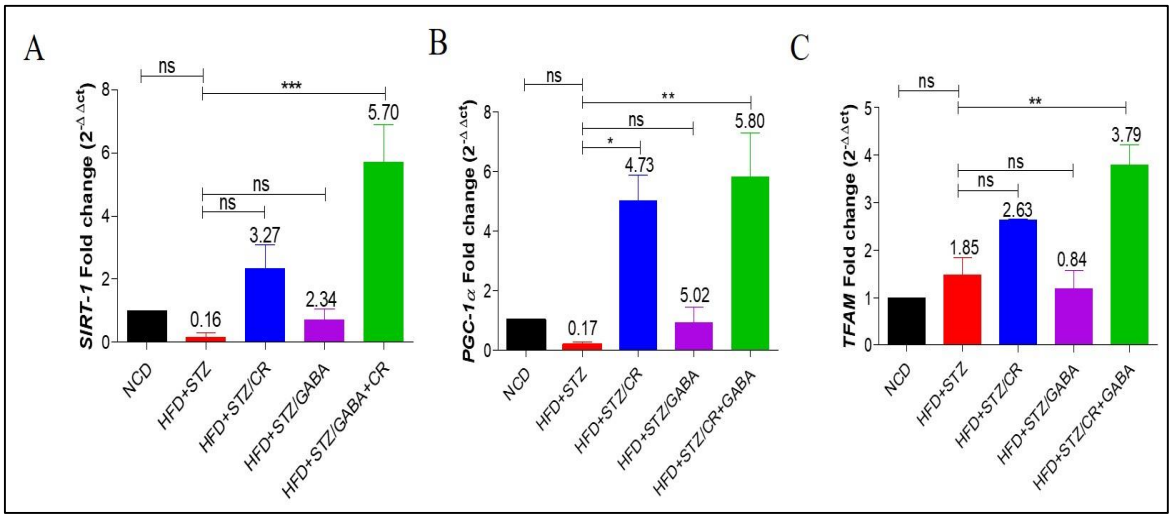

Figure 5.9 Transcript levels of mitochondrial biogenesis markers in the skeletal muscle. A) Fold change in ***SIRT-1* mRNA**. A 5.7 fold increase in *SIRT-1* expression was observed in CR+GABA treated group as compared to HFD+STZ group. B) ***PGC-1α* mRNA fold change**. A significant increase in *PGC-1* expression was observed in CR (4.7-fold) and CR+GABA (5.8-fold) treated groups as compared to HFD+STZ group. C) ***TFAM* mRNA fold change**. A significant increase in *TFAM* expression (3.7-fold) was observed in CR+GABA treated group as compared to HFD+STZ group. (*p<0.05, **p<0.01, ns=non-significant; p>0.05) (n=4-5/group).

5.3.3 Oxygen consumption rate

The rate of oxygen consumption is a significant indicator of mitochondrial activity. GABA group showed no significant difference in the ETC complex activities in skeletal muscle (p>0.05). CR fed mice showed significant increase (p<0.05) in OCR by ETC complex I compared to HFD+STZ group, indicating improved complex I activity in skeletal muscle. CR+GABA group showed significant OCR by ETC complexes I-III as compared to HFD+STZ group indicating improved complex activities in skeletal muscle (p<0.05) (Figure 5.10).

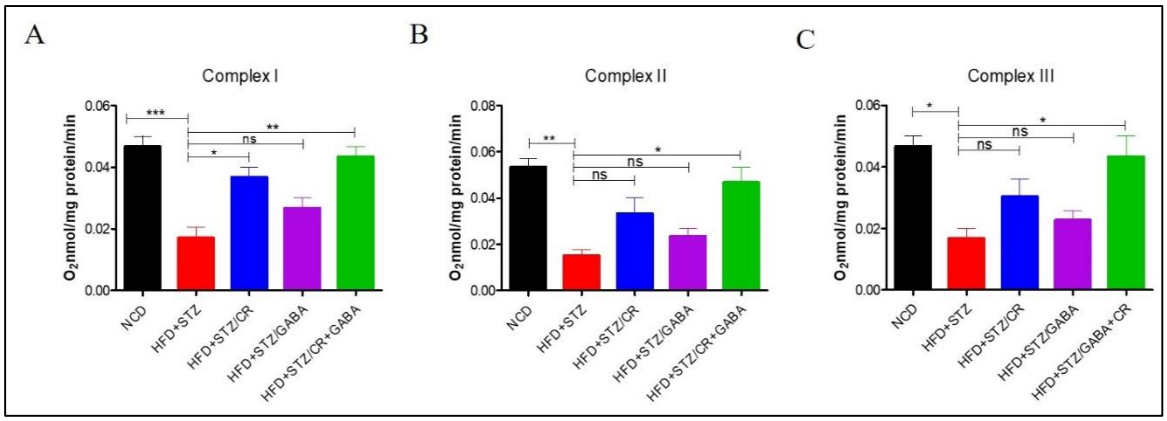

Figure 5.10 Estimation of OCR in skeletal muscle. The activities of complexes I-III were significantly reduced in the HFD+STZ group. A) CR and CR+GABA treated groups showed significant increase in complex I compared to HFD+STZ. B-C) CR+GABA treated group showed significant increase in complexes II and III activities compared to the HFD+STZ group. (ns=non-significant, *p<0.05, **p<0.01, ***p<0.001, n=4-5 group).

5.3.4 Pancreatic β-cell regeneration and apoptosis

β-cell proliferation and apoptosis were assessed by IHC microscopy. The GABA treated group showed significant increase in β-cell proliferation [BrdU/Insulin co-positive cells] (Figure 5.11 [1A-2A]) as compared to NCD (p<0.01) and HFD+STZ treated groups (p<0.001). A similar trend was observed for neogenesis [PDX-1/NGN-3/Insulin co-positive cells] (Figure 5.11[1B-2B]) as compared to NCD (p<0.001) and HFD+STZ treated groups (p<0.001). Also, GABA treated group showed significant reduction (p<0.01) in β-cell apoptosis [TUNEL positive cells] (Figure 5.11 [1D-2D]). However, the CR monotherapy group showed no β-cell regeneration, and there was no improvement in β-cell apoptosis (p>0.05) (Figure 5.11). The CR+GABA treated group showed significant increase as compared to NCD and HFD+STZ in β-cell proliferation (p<0.001; p<0.001) (Figure 5.11) and neogenesis (p<0.05; p<0.05) (Figure 5.11). The CR+GABA treated group showed significantly reduced β-cell apoptosis as compared to HFD+STZ (p<0.001) (Figure 5.11).

The GABA and CR monotherapies, along with GABA+CR group, did not show transdifferentiation (ARX/PAX4/Insulin co-positive cells) (p>0.05) (Figure 5.11).

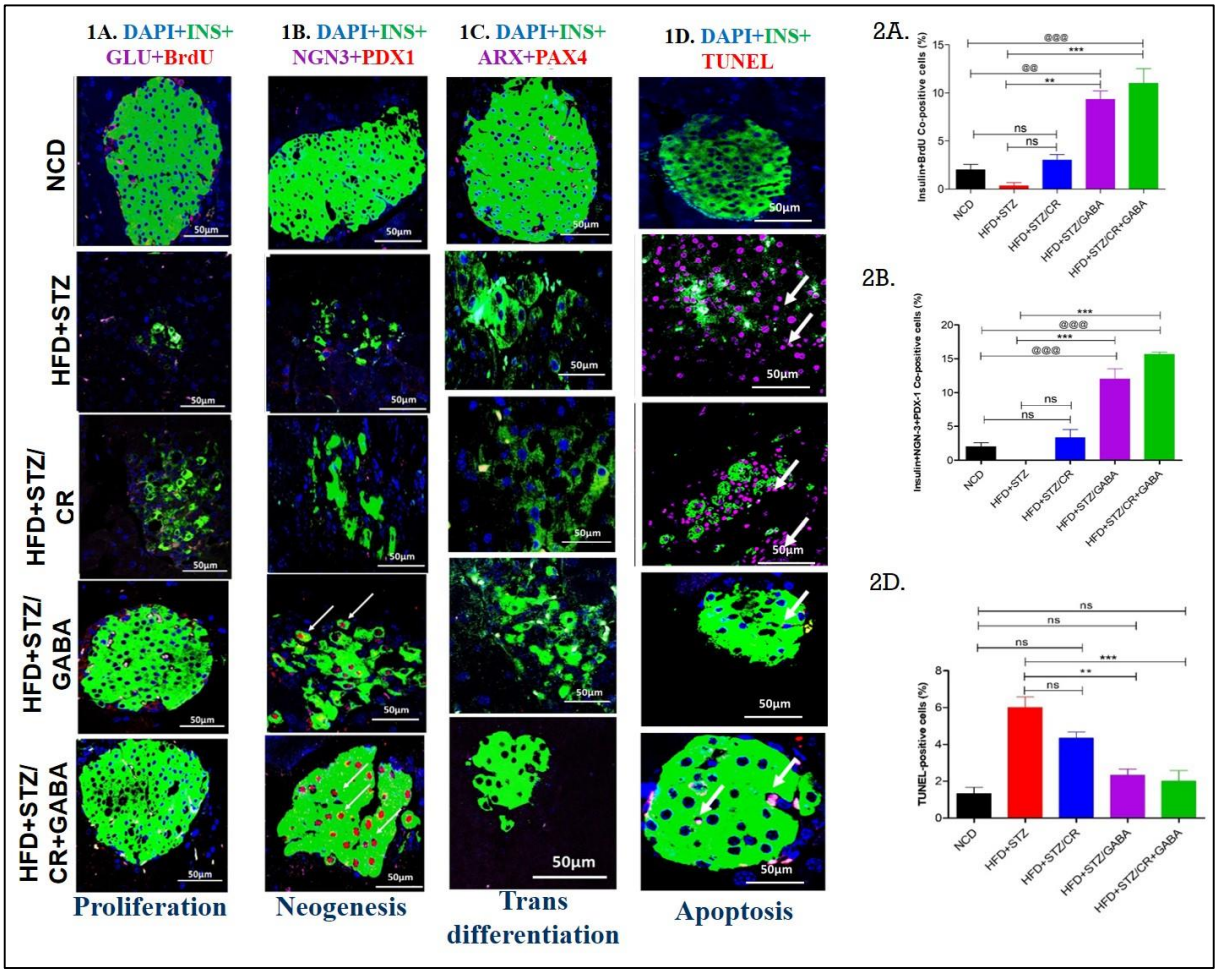

Figure 5.11 Assessment of pancreatic β-cell proliferation. (1A) Representative immunofluorescence images of pancreatic islets showing insulin (green), glucagon (magenta) and BrdU (red) cells in all the groups. (2A) Percentage of Insulin and BrdU co-positive cells. GABA and CR+GABA treated groups showed significant increase in β-cell proliferation as compared to HFD+STZ group. However, no significant difference was observed in CR group. (ns=non-significant, **p<0.01, ***p<0.001 vs HFD+STZ; $^{@@}p$<0.01, $^{@@@}p$<0.001 vs NCD; n=3/ group). **Assessment of pancreatic β-cell neogenesis. (1B)** Representative immunofluorescence images of pancreatic islets showing insulin (green), NGN-3 (magenta) and PDX-1 (red) cells in all the groups. (2B) Percent of Insulin, NGN-3 and PDX-1 co-positive cells. GABA and CR+GABA treated groups showed significant increase in β-cell neogenesis as compared to HFD+STZ group. However, no significant difference was observed in CR group. (ns=non-significant, *p<0.05 vs HFD+STZ; n=3/ group). **Assessment of pancreatic β-cell transdifferentiation. (1C)** Representative immunofluorescence images of pancreatic islets showing insulin (green),

ARX-1 (magenta) and PAX-4 (red) cells in all the groups. (ns=non-significant; n=3/ group). **Assessment of pancreatic β-cell apoptosis:** (1D) Representative immunofluorescence images of pancreatic islets, showing insulin (green) and TUNEL (red) cells in all the groups. (2D) Percent of Insulin and TUNEL co-positive cells. A significant reduction in β-cell apoptosis was observed in GABA and CR+GABA groups compared to HFD+STZ group. (ns=non-significant, $**p<0.01$, $***p<0.001$ vs HFD+STZ; n=3/group).

5.4 Discussion

The management of T2D involves two main approaches: i) increasing insulin secretion from the β-cells and ii) increasing insulin-mediated glucose uptake by the peripheral tissues. Patients develop tolerance against the existing line of treatment within a few years, which poses a challenge for developing new medicines. These drugs also show many side-effects [Rathwa *et al.*, 2020]. Thus, combination therapies involving naturally existing biomolecules are the way forward to overcome the complications of T2D. Therefore, the present study was designed to determine the therapeutic potential of a combination of CR and GABA in the T2D mouse model.

CR is a potential dietary intervention emphasizing caloric management in terms of fats, carbohydrates and proteins with sufficient vitamins and minerals. CR promotes insulin sensitivity, mitochondrial biogenesis and functionality [López-Lluch *et al.*, 2016; Golbidi *et al.*, 2017]. Mice fed with 30-40% of the ad libitum calorie deficit diet showed increased life expectancy, robustness against toxicity and stress [Fontana *et al.*, 2007]. Further data on similar lines showed CR reduced body weight and lipid profile markers when the therapy was prolonged [Huang *et al.*, 2010]. Several reports have explained CR as an activator of the SIRT1-PGC-1α signalling pathway at the transcriptional level [Smith *et al.*, 2009]. CR modulates lipid metabolism via the SIRT-1 signalling pathway and reduces intracellular DAG species [Baumeier *et al.*, 2015]. In the liver, PGC-1α may regulate the gluconeogenic pathway; however, the molecular mechanism remains unknown [Rodgers *et al.*, 2005].

Interestingly, we have also seen similar results at various levels with CR monotherapy reducing body weight and triglyceride levels and improving insulin sensitivity besides reducing gluconeogenesis and glycogenolysis. Civitarese *et al.* studied the molecular mechanism of CR in mitochondrial functionality showing increased mRNA expression of the genes involved in mitochondrial biogenesis (viz. SIRT1, PGC-1α and TFAM), with SIRT1 being the direct regulator of the pathway [Civitarese *et al.*, 2007]. Our studies also

showed increased mitochondrial biogenesis and oxygen consumption rate by ETC complex I in CR group which are in agreement with their findings.

GABA has a proven role in islet-cell hormone homeostasis, preserving the β-cell mass, suppressing unwanted immune reactions and consequent apoptosis [Wang *et al.,* 2019; Rathwa *et al.,* 2019]. The food sources of GABA are potatoes, tomatoes, and brown rice, while microorganisms like *E. coli, Lactococcus lactis* produce it [Oh *et al.,* 2003]. In the present study, GABA monotherapy effectively reduces FBG levels, improves glucose tolerance, increases insulin and c- peptide levels, reduces gluconeogenesis and glycogenolysis. GABAnergic system functions in many tissues, including the peripheral tissues. In the liver, $GABA_AR$ regulates PI3/Akt activities that maintain hepatocyte survival and PGC-1α expression. Thus, GABA is one of the multiple factors responsible for regulating hepatic glucose metabolism, i.e. gluconeogenic and glycogenolytic pathways [Wang *et al.,* 2017]. Fibroblast growth factor 21 (FGF-21) predominantly expressed in the liver under normal condition also induces PGC-1α expression. It leads to the regulation of lipolysis in the adipose tissue resulting in liver-adipose tissue crosstalk [Ye *et al.,* 2017]. The positive effect of GABA treatment stands documented in T1D and T2D murine models. GABA therapy protects NOD animals from diabetes, and a similar effect is reported in various *in-vivo* models [Soltani *et al.,* 2011; Tian *et al.,* 2011]. Also, GABA regulates cytokine secretion from human PBMCs and suppresses β-cell-reactive CD8+ CTLs in T1D models [Wang *et al.,* 2019; Soltani *et al.,* 2011], proposing the role of GABA as an immunosuppressant. GABA reportedly acts as an inducer of α-to-β-like cell conversion *in-vivo* upon prolonged exposure in the STZ-induced T1D mouse model [Wang *et al.,* 2019]. Although no β-cell transdifferentiation is observed in our GABA-treated group, a significant increase in β-cell proliferation and neogenesis, and reduced β-cell apoptosis are observed. The individual effects of CR and GABA on the multiple pathways and tissues diminish the adverse actions of T2D pathophysiology when given in combination. Our results suggest that the combination treatment improves glucose homeostasis by increasing insulin sensitivity and glucose tolerance. CR enhances insulin sensitivity by improving the mitochondrial function at two levels, elevating the expression of SIRT1, PGC-1α and TFAM and increasing mitochondrial complex I-III activities. GABA therapy boosts insulin levels by inducing β-cell proliferation and neogenesis and contributes to the existing depositary. It also enhances the metabolic profile by reducing BW, FBG levels, triglycerides, total cholesterol, and LDL levels. As mentioned earlier, the liver-adipose tissue crosstalk regulates these pathways at the transcriptional level. CR+GABA treated group showed a

significant decrease in the expression of G6Pase and PEPCK (gluconeogenesis), GLUT2 and G6Pase (glycogenolysis), and an increase in glucokinase (glycolysis). Interestingly, lipogenesis seems up-regulated as marked by the increased ACC expression, and consequently, lipolysis also gets up-regulated as a compensatory mechanism as observed by the increased ATGL expression. CR+GABA treated group shows a significant increase in β-cell proliferation, neogenesis, and reduced β-cell apoptosis. We did not observe AIF translocation for β-cell apoptosis, a marker for caspase-independent cell death. Increased oxidative stress induced by STZ and low levels of antioxidant enzymes in the pancreatic cells activate caspase-9 and caspase-3 leading to β-cell apoptosis [Al Nahdi *et al.*, 2017; Li *et al.*, 2014; Kostic *et al.*, 2020]. Hence, the HFD+STZ model mimics caspase-dependent β-cell apoptosis. However, further validation is required for caspase mediated cell death pathways.

However, there are a few limitations of this study: first, we used CR as one of our therapies and monitor parameters at the transcriptional level in different peripheral tissues. As CR is first-line therapy, it is ideal for assessing energy expenditure parameters which we have not studied. Second, we have not performed cell lineage tracing studies to establish GABA's role in β-cell regeneration. Thus, extensive *in vitro* and *in vivo* investigations are needed to address the above questions and whether the effect was due to the two different signalling cascades additive stimulus or an undefined underlying mechanism. Thus, the current study suggests that combination therapy with CR and GABA showed amelioration of pathophysiology in the T2D mouse model (Figure 5.12).

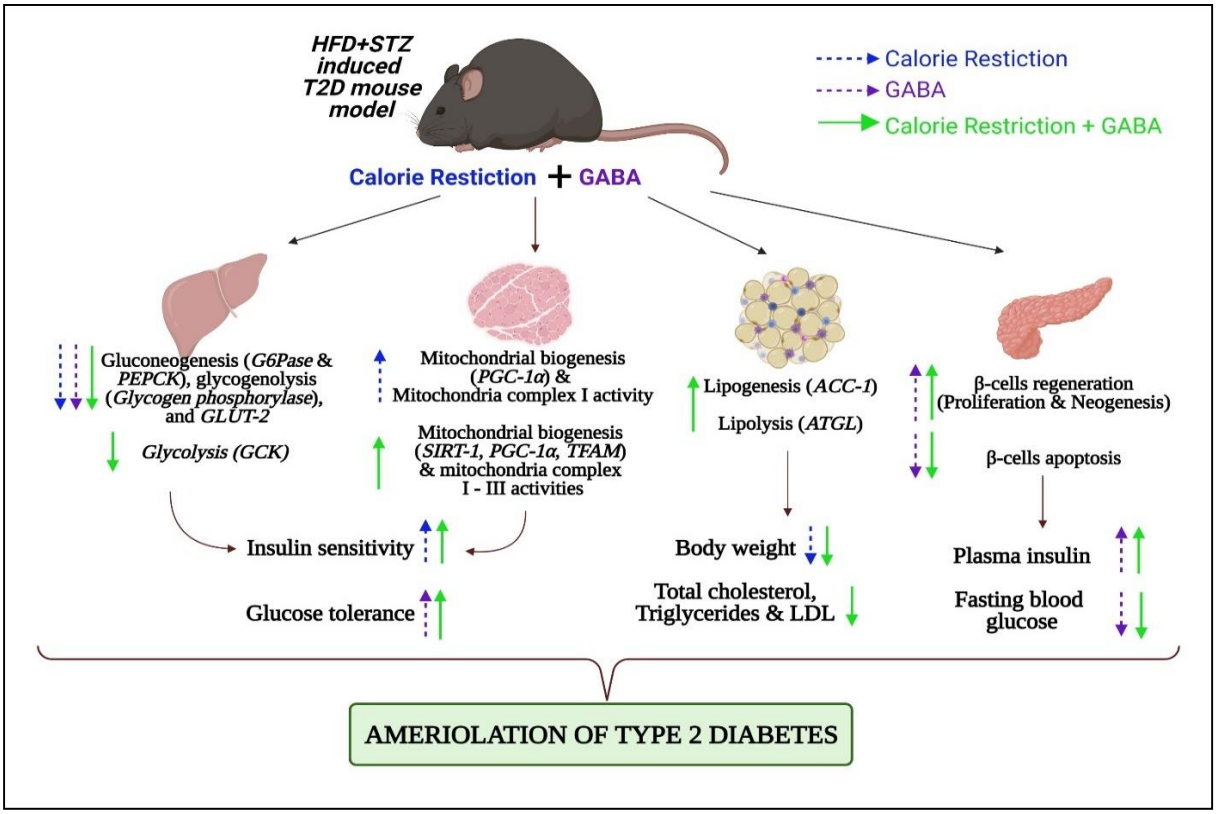

Figure 5.12 The effect of GABA, CR and CR+GABA (combination therapy) on amelioration of T2D pathophysiology in HFD+STZ induced T2D mouse model.

T2D pathophysiology is characterised by insulin resistance and β-cell loss. GABA monotherapy shows reduced FBG levels, improved insulin sensitivity and glucose tolerance, increased insulin and c-peptide levels, decreased gluconeogenesis and glycogenolysis. The GABA treated group also shows a significant increase in β-cell proliferation and neogenesis with significant reduction in β-cell apoptosis. CR diet-fed mice show reduced body weight and triglyceride levels, along with improved insulin sensitivity, reduced gluconeogenesis and glycogenolysis. They also show elevated expression of mitochondrial biogenesis markers and oxygen consumption rate by ETC complex I-III compared to the HFD+STZ group. CR diet-fed mice show no β-cell regeneration and no improvement in β-cell apoptosis as compared to the HFD+STZ group. GABA+CR treated group shows improved glucose homeostasis by increasing insulin sensitivity and glucose tolerance, enhancing the transcript levels of key markers of glucoregulatory enzymes and lipid metabolism, increasing mitochondrial biogenesis and ETC complex activities. Further, the combination treatment promotes β-cell regeneration and reduces β-cell apoptosis as compared to the HFD+STZ group.

References:

1. Al Nahdi AM, John A, Raza H. Elucidation of molecular mechanisms of streptozotocin-induced oxidative stress, apoptosis, and mitochondrial dysfunction in Rin-5F pancreatic β-cells. Oxidative Medicine and Cellular Longevity. 2017;2017.
2. Bansal P, Paul P, Mudgal J, Nayak PG, Pannakal ST, Priyadarsini KI, Unnikrishnan MK. Antidiabetic, antihyperlipidemic and antioxidant effects of the flavonoid rich fraction of Pilea microphylla (L.) in high fat diet/streptozotocin-induced diabetes in mice. Experimental and Toxicologic Pathology. 2012;64(6):651-8.
3. Baumeier C, Kaiser D, Heeren J, Scheja L, John C, Weise C, Eravci M, Lagerpusch M, Schulze G, Joost HG, Schwenk RW. Caloric restriction and intermittent fasting alter hepatic lipid droplet proteome and diacylglycerol species and prevent diabetes in NZO mice. Biochimica et Biophysica Acta (BBA)-Molecular and Cell Biology of Lipids. 2015;1851(5):566-76.
4. Ben-Othman N, Vieira A, Courtney M, Record F, Gjernes E, Avolio F, Hadzic B, Druelle N, Napolitano T, Navarro-Sanz S, Silvano S. Long-term GABA administration induces alpha cell-mediated beta-like cell neogenesis. Cell. 2017;168(1-2):73-85.
5. Bowe JE, Franklin ZJ, Hauge-Evans AC, King AJ, Persaud SJ, Jones PM. Metabolic phenotyping guidelines: assessing glucose homeostasis in rodent models. Journal of endocrinology. 2014;222(3):G13-25.
6. Civitarese AE, Carling S, Heilbronn LK, Hulver MH, Ukropcova B, Deutsch WA, Smith SR, Ravussin E. Calorie restriction increases muscle mitochondrial biogenesis in healthy humans. PLoS med. 2007;4(3):e76.
7. Dogan S, Ray A, Cleary MP. The influence of different calorie restriction protocols on serum pro-inflammatory cytokines, adipokines and IGF-I levels in female C57BL6 mice: short term and long term diet effects. Meta gene. 2017;12:22-32.
8. Dwivedi M, Laddha NC, Imran M, Ansarullah, Bajpai P, Ramachandran AV, Misra A, Yadav M, Begum R. ACE gene I/D polymorphism in type 2 diabetes: the Gujarat population. The British Journal of Diabetes & Vascular Disease. 2011;11(3):153-4.
9. Fontana L, Klein S. Aging, adiposity, and calorie restriction. Jama. 2007;297(9):986-94.
10. Fontana L, Partridge L. Promoting health and longevity through diet: from model organisms to humans. Cell. 2015;161(1):106-18.
11. Golbidi S, Daiber A, Korac B, Li H, Essop MF, Laher I. Health benefits of fasting and caloric restriction. Current diabetes reports. 2017 Dec;17(12):1-1.

12. Huang P, Li S, Shao M, Qi Q, Zhao F, You J, Mao T, Li W, Yan Z, Liu Y. Calorie restriction and endurance exercise share potent anti-inflammatory function in adipose tissues in ameliorating diet-induced obesity and insulin resistance in mice. Nutrition & metabolism. 2010;7(1):1-9.
13. Kadam A, Mehta D, Jubin T, Mansuri MS, Begum R. Apoptosis inducing factor: Cellular protective function in Dictyostelium discoideum. Biochimica et Biophysica Acta (BBA)-Bioenergetics. 2020;1861(5-6):148158.
14. Kostic S, Hauke T, Ghahramani N, Filipovic N, Vukojevic K. Expression pattern of apoptosis-inducing factor in the kidneys of streptozotocin-induced diabetic rats. Acta Histochemica. 2020;122(8):151655.
15. Li, Z., & Graham, B. H. (2012). Measurement of mitochondrial oxygen consumption using a Clark electrode. In Mitochondrial Disorders (pp. 63-72). Humana Press.
16. Li K, Wu D, Chen X, Zhang T, Zhang L, Yi Y, Miao Z, Jin N, Bi X, Wang H, Xu J. Current and emerging biomarkers of cell death in human disease. BioMed research international. 2014;2014(1):60-72.
17. López-Lluch G, Navas P. Calorie restriction as an intervention in ageing. The Journal of physiology. 2016;594(8):2043-60.
18. Oh SH, Moon YJ, Oh CH. γ-Aminobutyric acid (GABA) content of selected uncooked foods. Preventive Nutrition and Food Science. 2003;8(1):75-8.
19. Patel R, Dwivedi M, Mansuri MS, Laddha NC, Thakker A, Ramachandran AV, Begum R. Association of neuropeptide-Y (NPY) and interleukin-1beta (IL1B), genotype-phenotype correlation and plasma lipids with Type-II diabetes. PloS one. 2016;11(10):e0164437.
20. Patel R, Palit SP, Rathwa N, Ramachandran AV, Begum R. Genetic variants of tumor necrosis factor-α and its levels: A correlation with dyslipidemia and type 2 diabetes susceptibility. Clinical nutrition. 2019;38(3):1414-22.
21. Palit SP, Patel R, Jadeja SD, Rathwa N, Mahajan A, Ramachandran AV, Dhar MK, Sharma S, Begum R. A genetic analysis identifies a haplotype at adiponectin locus: association with obesity and type 2 diabetes. Scientific reports. 2020;10(1):1-0.
22. Pramanik S, Rathwa N, Patel R, Ramachandran AV, Begum R. Treatment avenues for type 2 diabetes and current perspectives on adipokines. Current diabetes reviews. 2018;14(3):201-21.

23. Picca A, Lezza AM. Regulation of mitochondrial biogenesis through TFAM–mitochondrial DNA interactions: useful insights from aging and calorie restriction studies. Mitochondrion. 2015;25:67-75.
24. Purwana I, Zheng J, Li X, Deurloo M, Son DO, Zhang Z, Liang C, Shen E, Tadkase A, Feng ZP, Li Y. GABA promotes human β-cell proliferation and modulates glucose homeostasis. Diabetes. 2014;63(12):4197-205.
25. Rathwa N, Patel R, Palit SP, Parmar N, Rana S, Ansari MI, Ramachandran AV, Begum R. β-cell replenishment: Possible curative approaches for diabetes mellitus. Nutrition, Metabolism and Cardiovascular Diseases. 2020;30(11):1870-81.
26. Rathwa NN, Patel R, Pramanik S, Parmar NR, Ramachandran A, Begum R. 143-LB: Calorie Restriction in Combination with GABA Ameliorates Type 2 Diabetes.2019
27. Rathwa N, Patel R, Palit SP, Ramachandran AV, Begum R. Genetic variants of resistin and its plasma levels: Association with obesity and dyslipidemia related to type 2 diabetes susceptibility. Genomics. 2019;111(4):980-5.
28. Rathwa N, Parmar N, Palit SP, Patel R, Ramachandran AV, Begum R. Intron specific polymorphic site of vaspin gene along with vaspin circulatory levels can influence pathophysiology of type 2 diabetes. Life sciences. 2020;243:117285.
29. Rodgers JT, Lerin C, Haas W, Gygi SP, Spiegelman BM, Puigserver P. Nutrient control of glucose homeostasis through a complex of PGC-1α and SIRT1. Nature. 2005;434(7029):113-8.
30. Smith JJ, Kenney RD, Gagne DJ, Frushour BP, Ladd W, Galonek HL, Israelian K, Song J, Razvadauskaite G, Lynch AV, Carney DP. Small molecule activators of SIRT1 replicate signaling pathways triggered by calorie restriction in vivo. BMC systems biology. 2009;3(1):1-4.
31. Soltani N, Qiu H, Aleksic M, Glinka Y, Zhao F, Liu R, Li Y, Zhang N, Chakrabarti R, Ng T, Jin T. GABA exerts protective and regenerative effects on islet beta cells and reverses diabetes. Proceedings of the National Academy of Sciences. 2011;108(28):11692-7.
32. Stoscheck CM. Quantitation of protein. Methods in enzymology. 1990 Jan 1;182:50-69.
33. Tian J, Dang H, Kaufman DL. Combining antigen-based therapy with GABA treatment synergistically prolongs survival of transplanted ß-cells in diabetic NOD mice. PloS one. 2011;6(9):e25337.

34. Wang Q, Ren L, Wan Y, Prud'homme GJ. GABAergic regulation of pancreatic islet cells: physiology and antidiabetic effects. Journal of cellular physiology. 2019;234(9):14432-44.
35. Wang S, Xiang YY, Zhu J, Yi F, Li J, Liu C, Lu WY. Protective roles of hepatic GABA signaling in acute liver injury of rats. American Journal of Physiology-Gastrointestinal and Liver Physiology. 2017;312(3):G208-18.
36. Ye DW, Rong XL, Xu AM, Guo J. Liver-adipose tissue crosstalk: A key player in the pathogenesis of glucolipid metabolic disease. Chinese journal of integrative medicine. 2017;23(6):410-4.

CONCLUSIONS

Conclusions

Diabetes Mellitus is a metabolic disorder characterized by persistent hyperglycemia. Autoimmune-mediated destruction of pancreatic β-cells causes type 1 diabetes (T1D). On the contrary, type 2 diabetes (T2D) is manifested by insulin resistance in peripheral tissues due to impaired insulin signalling. T2D is caused by a combination of genetic and lifestyle factors such as diet, obesity, lack of exercise and ER stress. Adipose tissue secretes pro- and anti-inflammatory adipokines such as resistin, omentin-1 and vaspin, which are in a state of equilibrium. They play an essential role in regulating metabolism, insulin sensitivity and satiety. The pharmacological interventions for T2D involve two methods: i) insulin secretion from β-cells and ii) insulin-mediated glucose uptake from peripheral tissues. The existing therapies only help improve hyperglycemia and other symptomatic characteristics. Since glucose control can thwart the devastating complications of diabetes, research now focuses on β-cell regeneration. In our population based study, genetic variants of *resistin, omentin-1* and *vaspin* with their altered transcript/protein levels were evaluated to understand the underlying mechanism of adipokines in the development of obesity-induced T2D. Our present work further explores the combined effect of CR and GABA in the amelioration of T2D pathophysiology in T2D mouse model.

Our population study based findings suggest *resistin* rs1862513 C/G polymorphism and *vaspin* rs2274907 A/T polymorphism could pose a risk towards T2D susceptibility. Moreover, increased plasma resistin protein levels, decreased plasma omentin-1 and vaspin protein levels, and associated metabolic alterations might play a role in developing T2D risk in the Gujarat population. We have also evaluated the efficacy of CR, GABA and combination therapy in HFD+STZ induced T2D mouse model. Our results showed amelioration of T2D by inducing β-cell proliferation and reduced β-cell apoptosis; glucose homeostasis by increasing insulin sensitivity; glucose tolerance by improving transcript levels of key metabolic markers, mitochondrial biogenesis and ETC complex activities (Fig 7). Our study suggests that CR and GABA combination therapy could help overcome T2D pathophysiology by their action at multiple sites, regulating glucose and lipid metabolism. CR treatment seems part of a first-line therapy that can be used with other drugs like DPP-IV inhibitors or metformin. Moreover, a CR-mimetic, for instance, resveratrol, is available commercially to easily overcome the challenge of strict dietary regimen and protocols. GABA monotherapy works on β-cell regeneration, readily available from natural sources like spinach and tomatoes. An edible vegetable extract can be formulated for diabetic patients

without manifestation of significant side effects. Thus, combination therapy can be helpful to combat T2D pathophysiology. However, this study needs further investigation at pre-clinical and clinical levels to evaluate the commercial viability.

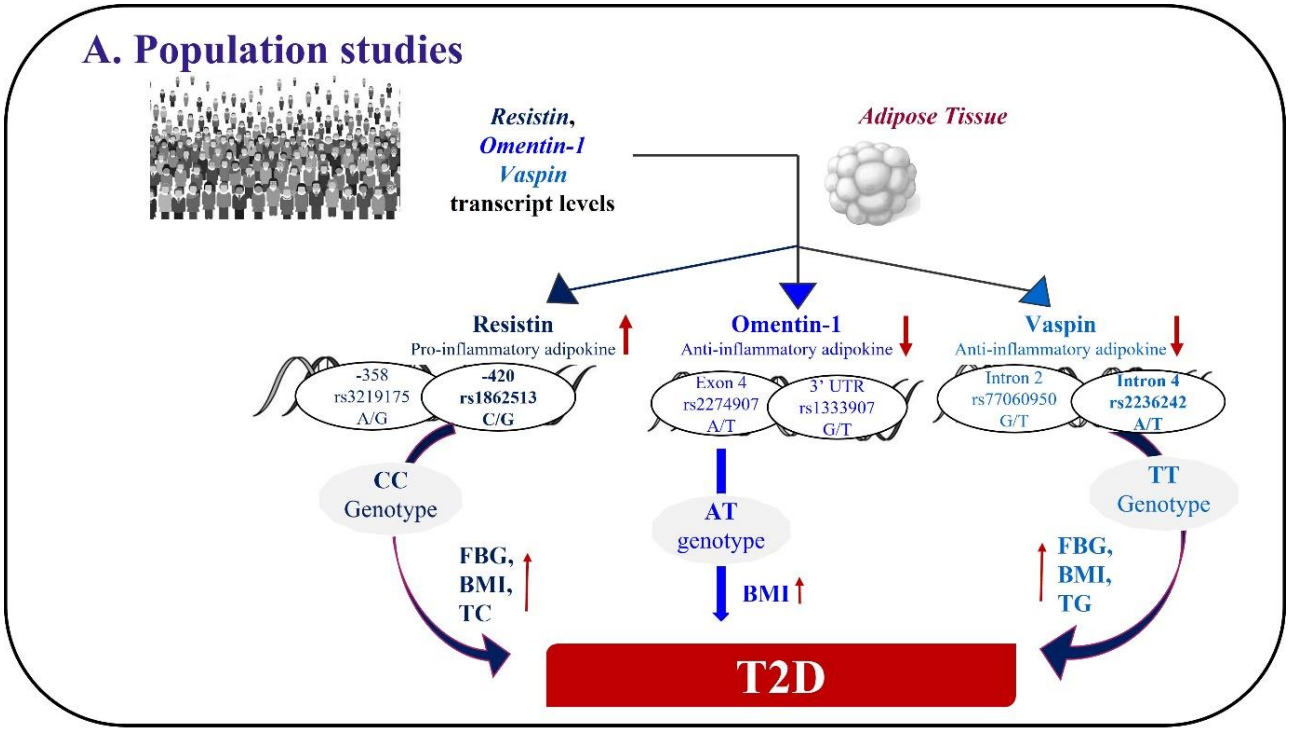

Figure 7.1 The role of resistin, omentin-1 and vaspin in development of T2D: *Resistin* rs1862513 C/G polymorphism is strongly associated with elevated resistin levels and increased BMI, FBG and TC levels. *Omentin-1* genetic variants are not associated with T2D but reduced protein levels are observed in T2D. *Vaspin* rs2274907 A/T polymorphism is strongly associated with its reduced transcript and protein levels. These metabolic alterations may play a role in the development of T2D.

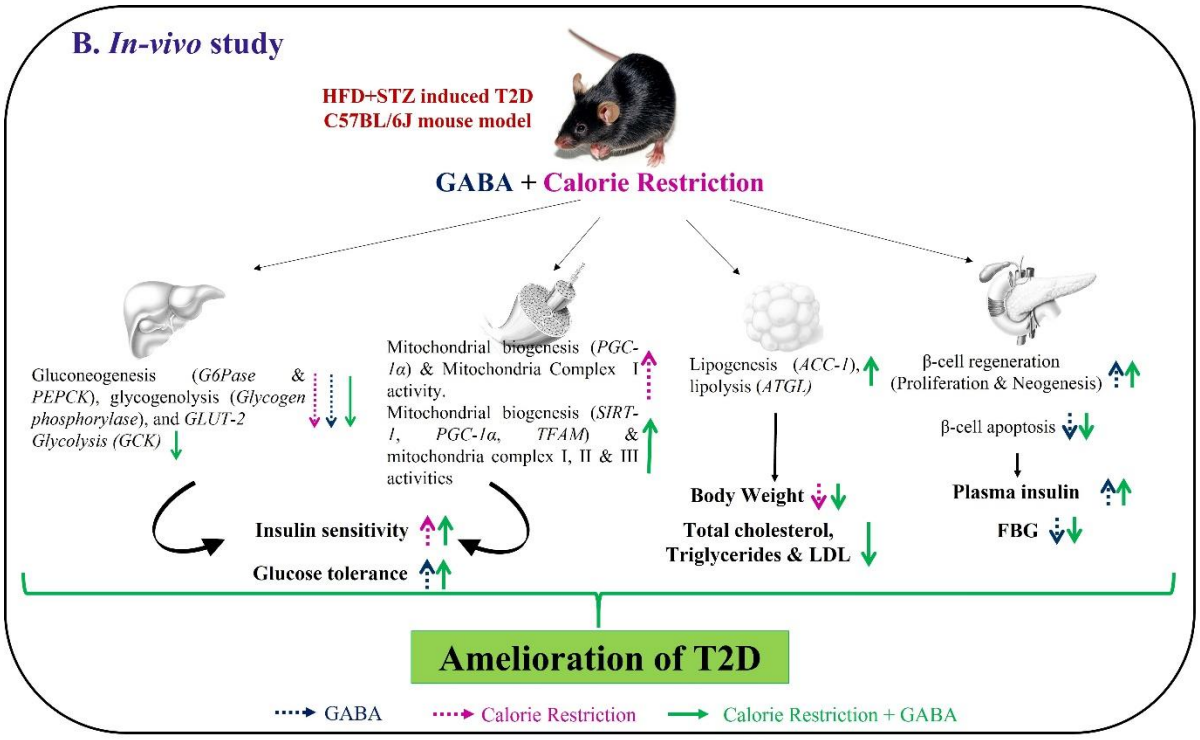

Figure 7.2 Effect of GABA, CR and CR+GABA (combination therapy) in amelioration of T2D pathophysiology in HFD+STZ induced T2D mouse model. T2D pathophysiology is characterised by insulin resistance and β-cell loss. GABA monotherapy shows reduced FBG levels, improved insulin sensitivity and glucose tolerance, increased insulin and c-peptide levels and decreased gluconeogenesis and glycogenolysis compared to HFD+STZ group. The GABA treated group also shows significant increase in β-cell proliferation and neogenesis with significantly reduced β-cell apoptosis. CR diet-fed mice show reduced body weight and triglycerides levels, along with improved insulin sensitivity, reduced gluconeogenesis and glycogenolysis. CR group also show elevated expression of mitochondrial biogenesis markers and oxygen consumption rate by ETC complexes I-III compared to HFD+STZ group. CR diet-fed mice show no β-cell regeneration and no improvement in β-cell apoptosis compared to HFD+STZ group. GABA+CR treated group shows improved glucose homeostasis by increasing insulin sensitivity and glucose tolerance, enhancing the transcript levels of key markers of glucoregulatory enzymes and lipid metabolism, and increasing mitochondrial biogenesis and ETC complex activities. Further, the combination therapy promotes β-cell regeneration and reduces β-cell apoptosis as compared to HFD+STZ group.